

REPORT DOCUMENTATION PAGE				Form Approved OMB No. 0704-0188	
Public reporting burden for this collection of information is estimated to average 1 hour per response, including the time for reviewing instructions, searching existing data sources, gathering and maintaining the data needed, and completing and reviewing this collection of information. Send comments regarding this burden estimate or any other aspect of this collection of information, including suggestions for reducing this burden to Department of Defense, Washington Headquarters Services, Directorate for Information Operations and Reports (0704-0188), 1215 Jefferson Davis Highway, Suite 1204, Arlington, VA 22202-4302. Respondents should be aware that notwithstanding any other provision of law, no person shall be subject to any penalty for failing to comply with a collection of information if it does not display a currently valid OMB control number. PLEASE DO NOT RETURN YOUR FORM TO THE ABOVE ADDRESS.					
1. REPORT DATE (DD-MM-YYYY) 19-02-2008		2. REPORT TYPE Journal Article		3. DATES COVERED (From - To)	
4. TITLE AND SUBTITLE Liquid Azide Salts and Their Reactions with Common Oxidizers IRFNA and N ₂ O ₄ (Postprint)				5a. CONTRACT NUMBER	
				5b. GRANT NUMBER	
				5c. PROGRAM ELEMENT NUMBER	
6. AUTHOR(S) Stefan Schneider, Michael Rosander, & Steven Chambreau (ERC); Tommy Hawkins, Jeffrey Mills, & Ghanshyam Vaghjiani (AFRL/RZSP)				5d. PROJECT NUMBER 23030423	
				5e. TASK NUMBER	
				5f. WORK UNIT NUMBER	
7. PERFORMING ORGANIZATION NAME(S) AND ADDRESS(ES) Air Force Research Laboratory (AFMC) AFRL/RZSP 10 E. Saturn Blvd. Edwards AFB CA 93524-7680				8. PERFORMING ORGANIZATION REPORT NUMBER AFRL-RZ-ED-JA-2008-051	
9. SPONSORING / MONITORING AGENCY NAME(S) AND ADDRESS(ES) Air Force Research Laboratory (AFMC) AFRL/RZS 5 Pollux Drive Edwards AFB CA 93524-70448				10. SPONSOR/MONITOR'S ACRONYM(S)	
				11. SPONSOR/MONITOR'S NUMBER(S) AFRL-RZ-ED-JA-2008-051	
12. DISTRIBUTION / AVAILABILITY STATEMENT Approved for public release; distribution unlimited (PA# 08087A)					
13. SUPPLEMENTARY NOTES Published in <i>Inorganic Chemistry</i> , 2008, 47, 6082-6089. (c) 2008 American Chemical Society.					
14. ABSTRACT Several imidazolium-based ionic liquid azides with saturated and unsaturated side chains were prepared and their physical and structural properties were investigated. The reactivity of these new as well as some previously reported ionic liquid azides with the strong oxidizers, N ₂ O ₄ and inhibited, red-fuming-nitric acid (IRFNA), were studied.					
15. SUBJECT TERMS					
16. SECURITY CLASSIFICATION OF:			17. LIMITATION OF ABSTRACT SAR	18. NUMBER OF PAGES 9	19a. NAME OF RESPONSIBLE PERSON Dr. Tommy Hawkins
a. REPORT Unclassified	b. ABSTRACT Unclassified	c. THIS PAGE Unclassified			19b. TELEPHONE NUMBER (include area code) N/A

Liquid Azide Salts and Their Reactions with Common Oxidizers IRFNA and N₂O₄

Stefan Schneider,* Tommy Hawkins, Michael Rosander, Jeffrey Mills, Ghanshyam Vaghjiani, and Steven Chambeau

Space and Missile Propulsion Division, 10 East Saturn Boulevard, Air Force Research Laboratory, Edwards Air Force Base, California 93524

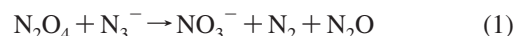
Received March 14, 2008

Several imidazolium-based ionic liquid azides with saturated and unsaturated side chains were prepared, and their physical and structural properties were investigated. The reactivity of these new as well as some previously reported ionic liquid azides with strong oxidizers, N₂O₄ and inhibited, red-fuming-nitric acid (IRFNA), was studied.

Introduction

Ethylammonium nitrate is commonly regarded as the first reported room-temperature ionic liquid (IL),¹ and was discovered after two closely related compounds, hydroxyethylammonium nitrate² and hydrazinium azide.³ With melting points of 52–55 and 75 °C, respectively, these salts still qualify as ILs according to the common definition: a salt with a melting point at or below 100 °C. It is interesting to note that these materials not only are ILs but also are energetic ILs and have been used in both explosive and propellant applications.^{4–6} A propellant containing hydrazinium azide was test-fired and spontaneous ignition was achieved upon contact with inhibited, red-fuming nitric acid (IRFNA).⁷ This is commonly referred to as hypergolic ignition and is very desirable for bipropellant applications because of its relative engineering simplicity and reliability.⁸ Consequently, we became interested in the reactivity of recently described IL azides⁹ with commonly used oxidizers such as IRFNA and N₂O₄. The latter was of particular interest

because it is known that the azide anion reacts completely with N₂O₄ to yield only nitrates and lightweight gases N₂ and N₂O (eq 1).



This reaction is thought to proceed through an unstable intermediate, NON₃, which has been the subject of multiple investigations.^{10–12} If the N₃[−]/N₂O₄ reaction provides enough heat to ignite a salt with a heterocyclic cation and an azide anion, these materials could be candidates as replacements for hydrazine in bipropellant applications.

The priority placed on finding a suitable replacement for the fuel component in bipropellant applications can be illustrated with the N₂H₄/N₂O₄ system. The dangers and operational costs associated with other methylated hydrazine fuels and nitrogen-containing oxidizers are similar.

Although NO₂ and N₂O₄ are acute toxins, neither is listed by the IARC (International Agency for Research on Cancer), NTP (National Toxicology Program), or OSHA (Occupational Safety and Health Administration) as a carcinogen or potential carcinogen, as is hydrazine. The working concentrations permitted for NO_x (3 ppm) are substantially higher than those for hydrazine (0.01 ppm). In addition, nitrogen oxides can be detected by their odor at levels considerably below the danger limits. In contrast, hydrazine cannot be detected by the human nose until levels are nearly 400 times the recommended safe concentrations. Hydrazine toxicity and containment are further exacerbated by its high vapor

(10) Schulz, A.; Tornieporth-Oetting, I. C.; Klapötke, T. *Angew. Chem., Int. Ed. Engl.* **1993**, 32, 1610.

(11) Doyle, M. P.; Maciejko, J. J.; Busman, S. C. *J. Am. Chem. Soc.* **1973**, 95, 952.

(12) Lucien, H. W. *J. Am. Chem. Soc.* **1958**, 80, 4458.

* To whom correspondence should be addressed. Fax: +1-661-275-5471. E-mail: stefan.schneider@edwards.af.mil.

(1) Walden, P. *Bull. Acad. Imp. Sci.* **1914**, 1800.

(2) Gabriel, S. *Ber. Dtsch. Chem. Ges.* **1888**, 21, 2664.

(3) Curtius, T. *Ber. Dtsch. Chem. Ges.* **1891**, 24, 3341.

(4) Minnick, J. J. U.S. Patent US3409484, 1968.

(5) Duglison, C.; Lyster, W. M. U.S. Patent US3431155, 1969.

(6) Koch, J. H. German Patent GE1117015, 1961; U.S. Patent US3066479, 1962; U.K. Patent UK920518, 1963.

(7) Schmidt, E. W. *Hydrazine and Its Derivatives*, 2nd ed.; Wiley: New York, 2001; pp 1470–1472.

(8) Clark, J. D. *Ignition!*, Rutgers University Press: New Brunswick, NJ, 1972.

(9) Schneider, S.; Hawkins, T.; Rosander, M.; Mills, J. D.; Brand, A.; Hudgens, L.; Warmoth, G.; Vij, A. *Inorg. Chem.* **2008**, 47, 3617.

pressure (13.87 kPa at 20 °C). Therefore, replacing hydrazines with an IL, which generally possesses very low volatility and therefore virtually no vapor toxicity, would be extremely beneficial.

In addition to the currently reported imidazolium compounds, which were chosen to improve thermal stability, some previously reported amino-triazolium azides⁹ were screened for hypergolicity with N₂O₄ and IRFNA. The synthesis and structural and physical properties of some novel imidazolium azides with a variety of energetic and perhaps innately reactive, unsaturated side chains are discussed. In one instance, the crystalline product of reaction with N₂O₄ was recovered. Its precise composition was determined from an X-ray single crystal investigation.

Experimental Section

Caution! None of the prepared azides showed particular sensitivity toward friction (scratching with a metal spatula) or impact (hitting with a hammer), and no accidents or mishaps occurred during work with these materials. However, the use of appropriate safety precautions (safety shields, face shields, leather gloves, and protective clothing such as heavy leather welding suits and ear plugs) are mandatory for work with any energetic materials, especially when working on a larger scale. Ignoring safety precautions can lead to serious injuries!

All starting materials were purchased from Aldrich Chemical Co., Inc., and their purities were checked by ¹H and ¹³C NMR prior to use. Acetonitrile (99.93+% HPLC grade), methanol (99.93% ACS HPLC grade), diethyl ether (anhydrous, 99+%, ACS Reagent), and the azide exchange resin (azide on Amberlite IRA-400, 16–50 mesh ~3.8 mmol N₃/g) were used as received. The substituted imidazolium halides¹³ and the substituted triazolium azides⁹ were prepared according to literature procedures. Nonvolatile solids were handled in the dry nitrogen atmosphere of a glovebox. Raman spectra were recorded in the range 4000–80 cm⁻¹ on a Bruker Equinox 55 FT-RA 106/S spectrometer using a Nd:YAG laser at 1064 nm. Pyrex melting-point capillaries or 5 mm glass NMR tubes were used as sample containers. IR spectra were recorded on a Mattson Galaxy FTIR spectrometer using a glass, gas IR cell equipped with CsI windows. NMR spectra were recorded on a Bruker Spectrospin DRX 400 MHz Ultrashield spectrometer at room temperature with samples as neat liquids or dissolved in DMSO-*d*₆ using 5 mm NMR tubes. The ¹H and ¹³C spectra were referenced to external samples of neat TMS; ¹⁴N spectra were referenced to external samples of neat nitromethane. Melting points were determined by differential scanning calorimetry using a Thermal Analyst 200, Dupont 910 Differential Scanning Calorimeter. Measurements were carried out at a heating rate of 10 °C/min in sealed aluminum pans with a nitrogen flow rate of 20 mL/min. The reference sample was an empty Al container, which was sealed in the nitrogen atmosphere of a glovebox. Elemental analyses were performed on a PerkinElmer 2400 Series II CHNS/O elemental analysis instrument equipped with AD6 Autobalance. Viscosities were measured using a Brookfield RVDV-II+Pro viscometer equipped with a CPE-40 cone spindle at 10 RPM. The instrument was connected to a Brookfield TC-502 temperature controller set at 25 °C.

General Procedure for the Preparation of Imidazolium Salts (1–7). To a 100 mL Schlenk flask equipped with a Teflon stir bar and purged with nitrogen, the 1-*R*-3-methyl-imidazolium bromides were added and dissolved in ca. 30 mL of acetonitrile. A molar excess (up to 10 times) of azide exchange resin (3.8 mmol N₃/g) was added to the stirred solution, and stirring was continued for ~16 h. The insoluble polymeric reagent was removed by filtration, and the solvent was removed in a dynamic vacuum, leaving behind the corresponding IL azides.

1-Butyl-3-methyl-imidazolium Azide (1). 1-Butyl-3-methyl-imidazolium bromide (1.37 g) (6.24 mmol) and 8.21 g (31.20 mmol N₃⁻) of azide exchange resin were reacted. Obtained as a supercooled amber liquid, yield 95%; melting point (peak): +36 °C; decomp. onset +222 °C. Raman (375 mW, 25 °C, cm⁻¹) ν = 3149(5), 3076(8), 2955(47), 2940(44), 2913(38), 2873(33), 2830(8), 2736(4), 1566(5), 1446(12), 1416(20), 1385(12), 1319(41), 1244(8), 1210(2), 1172(1), 1116(6), 1055(4), 1021(17), 975(0+), 950(0+), 906(2), 883(4), 827(4), 810(3), 734(0+), 699(3), 658(2), 623(4), 600(6), 500(1), 416(3), 326(4), 85(100); δ_{1H} (neat liquid) 8.83 (1H, s), 7.39 (1H, s), 7.29 (1H, s), 3.69 (2H, t, CH₂CH₂CH₂CH₃, *J*_{H_z} 6.5), 3.43 (3H, s, CH₃), 1.15 (2H, quintet, CH₂CH₂CH₂CH₃, *J*_{H_z} 6.9) 0.54 (2H, sextet, CH₂CH₂CH₂CH₃, *J*_{H_z} 7.2), 0.12 (3H, t, CH₂CH₂CH₂CH₃, *J*_{H_z} 7.3); δ_{13C} (neat liquid) 137.6, 123.8, 122.6, 49.1, 35.4, 32.0, 19.2, 13.0; δ_{14N} (neat liquid ($\Delta_{1/2}$, Hz)) –132 (25), –194 (145), –209 (140), –280 (85). Found: C, 52.63; H, 8.52; N, 38.52. Calc. for C₈H₁₅N₅: C, 53.02; H, 8.34; N, 38.64.

1-Hydroxyethyl-3-methyl-imidazolium Azide (2). 1-Hydroxyethyl-3-methyl-imidazolium bromide (0.33 g) (1.73 mmol) and 0.68 g (2.58 mmol N₃⁻) of azide exchange resin were reacted. Obtained as a supercooled clear liquid, yield 95%; melting point (peak): +36 °C; decomp. onset +214 °C. Raman (400 mW, 25 °C, cm⁻¹) ν = 3160(7), 3098(8), 2957(44), 2886(13), 2834(7), 1565(4), 1452(7), 1417(19), 1386(8), 1334(21), 1247(3), 1196(1), 1075(4), 1022(16), 946(2), 874(4), 703(3), 652(1), 602(7), 495(4), 417(3), 331(2), 279(2), 85(100); δ_{1H} (DMSO-*d*₆) 9.13 (1H, s), 7.74 (1H, t, *J*_{H_z} 1.7), 7.71 (1H, t, *J*_{H_z} 1.7), 5.30 (1H, t, CH₂CH₂OH, *J*_{H_z} 5.0), 4.21 (2H, t, CH₂CH₂OH, *J*_{H_z} 4.8), 3.87 (3H, s, CH₃), 3.71 (2H, q, CH₂CH₂OH, *J*_{H_z} 4.9); δ_{13C} (DMSO-*d*₆) 137.3, 123.8, 123.1, 59.7, 52.0, 36.1; δ_{14N} (DMSO-*d*₆ ($\Delta_{1/2}$, Hz)) –131 (25), –210 (1300), –277 (145). Found: C, 42.59; H, 6.51; N, 40.89. Calc. for C₆H₁₁N₅O: C, 42.60; H, 6.55; N, 41.39.

1-Allyl-3-methyl-imidazolium Azide (3). 1-Allyl-3-methyl-imidazolium bromide (0.88 g) (4.36 mmol) and 13.24 g (50.31 mmol N₃⁻) of azide exchange resin were reacted. Dark amber liquid, yield 72%; melting point (peak): +19 °C; decomp. onset +150 °C. Raman (500 mW, 25 °C, cm⁻¹) ν = 3153(4), 3082(9), 3019(23), 2981(18), 2951(29), 2826(3), 2801(2), 1645(15), 1565(3), 1472(5), 1412(15), 1384(5), 1318(34), 1293(7), 1244(7), 1173(0+), 1107(2), 1021(12), 947(4), 918(1), 756(5), 676(3), 624(4), 569(3), 501(2), 459(2), 397(1), 318(0+), 103(80), 84(100); δ_{1H} (DMSO-*d*₆) 9.26 (1H, s), 7.79 (1H, t, *J*_{H_z} 1.6), 7.78 (1H, t, *J*_{H_z} 1.7), 6.05–5.98 (1H, m, CH₂CHCH₂), 5.31–5.26 (2H, m, CH₂CHCH₂), 4.88 (2H, d, CH₂CHCH₂, *J*_{H_z} 6.0), 3.89(3H, s, CH₃); δ_{13C} (DMSO-*d*₆) 137.2, 132.2, 124.2, 122.8, 120.6, 51.2, 36.0; δ_{14N} (DMSO-*d*₆ ($\Delta_{1/2}$, Hz)) –132 (130), –205 (270), –277 (280). Found: C, 50.87; H, 6.70; N, 42.21. Calc. for C₇H₁₁N₅: C, 50.90; H, 6.71; N, 42.39.

1-(3-Butenyl)-3-methyl-imidazolium Azide (4). 1-(3-Butenyl)-3-methyl-imidazolium bromide (0.70 g) (3.23 mmol) and 9.05 g (34.39 mmol N₃⁻) of azide exchange resin were reacted. Obtained as a supercooled dark amber liquid, yield 83%; melting point (peak): +45 °C; decomp. onset +188 °C. Raman (100 mW, 25 °C, cm⁻¹) ν = 3075(15), 3004(38), 2953(67), 2912(32), 1641(53), 1561(6), 1525(13), 1418(40), 1383(11), 1318(100), 1294(8), 1244(20),

(13) Schneider, S.; Drake, G.; Hall, L.; Hawkins, T.; Rosander, M. *Z. Anorg. Allg. Chem.* **2007**, *633*, 1701.

1109(1), 1021(33), 843(5), 600(13), 492(0+), 123(47); δ_{1H} (DMSO- d_6) 9.13 (1H, s), 7.76 (1H, t, J_{Hz} 1.7), 7.68 (1H, t, J_{Hz} 1.7), 5.77–5.70 (1H, m, $CH_2CH_2CHCH_2$), 5.05–5.00 (2H, m, $CH_2CH_2CHCH_2$), 4.25 (2H, t, J_{Hz} 6.8, $CH_2CH_2CHCH_2$), 3.84 (3H, s, CH_3), 2.55 (2H, d, J_{Hz} 6.8, $CH_2CH_2CHCH_2$); δ_{13C} (DMSO- d_6) 137.0, 134.0, 123.9, 122.8, 118.9, 48.4, 36.1, 34.0; δ_{14N} (DMSO- d_6 ($\Delta_{1/2}$, Hz)) –133 (40), –199 (160), –209 (168), –284 (159). Found: C, 53.58; H, 7.28; N, 38.91. Calc. for $C_8H_{13}N_5$: C, 53.61; H, 7.31; N, 39.08.

1-(2-Butynyl)-3-methyl-imidazolium Azide (5). 1-(2-Butynyl)-3-methyl-imidazolium bromide (1.15 g) (5.35 mmol) and 14.07 g (53.47 mmol N_3^-) of azide exchange resin were reacted. Solid, yield 65% (after recrystallization from methanol solution layered with diethyl ether); melting point (peak): +66 °C; decomp. onset +115 °C. Raman (500 mW, 25 °C, cm^{-1}) ν = 3098(7), 3074(7), 3015(15), 2959(30), 2917(51), 2741(4), 2324(6), 2248(36), 1569(5), 1459(9), 1425(13), 1408(24), 1381(21), 1329(21), 1322(49), 1267(1), 1243(11), 1174(5), 1106(7), 1088(6), 1020(20), 946(3), 883(4), 793(4), 748(9), 641(10), 629(9), 449(10), 403(12), 367(23), 322(13), 270(11), 196(21), 111(100), 84(83); δ_{1H} (methanol- d_4) 9.11 (1H, s), 7.71 (1H, d, J_{Hz} 2.0), 7.64 (1H, d, J_{Hz} 2.0), 5.10 (2H, q, J_{Hz} 2.5, CH_2CCCH_3), 3.99 (3H, s, CH_3), 1.94 (3H, t, J_{Hz} 2.4, CH_2CCCH_3); δ_{13C} (methanol- d_4) 136.2, 123.8, 121.9, 85.1, 69.5, 39.1, 35.2, 1.8; δ_{14N} (methanol- d_4 ($\Delta_{1/2}$, Hz)) –133 (60), –201 (116), –208 (120), –283 (186). Found: C, 54.12; H, 6.25; N, 38.89. Calc. for $C_8H_{11}N_5$: C, 54.22; H, 6.26; N, 39.52.

1-(2-Pentynyl)-3-methyl-imidazolium Azide (6). 1-(2-Pentynyl)-3-methyl-imidazolium bromide (1.40 g) (6.11 mmol) and 3.21 g (12.20 mmol N_3^-) of azide exchange resin were reacted. Dark amber liquid, yield 90%; melting point (peak): +19 °C; decomp. onset +107 °C. Raman (500 mW, 25 °C, cm^{-1}) ν = 3155(7), 3075(10), 2936(81), 2848(19), 2734(4), 2294(11), 2241(51), 1641(1), 1569(7), 1414(32), 1385(18), 1322(39), 1244(6), 1167(3), 1144(1), 1104(7), 1063(13), 1020(33), 961(11), 880(1), 756(7), 660(5), 636(6), 614(14), 512(4), 431(5), 401(10), 354(4), 271(12), 94(100); δ_{1H} (DMSO- d_6) 9.30 (1H, s), 7.80 (1H, s), 7.78 (1H, s), 5.18 (2H, s, $CH_2CCCH_2CH_3$), 3.89 (3H, s, CH_3), 2.29–2.24 (2H, m, $CH_2CCCH_2CH_3$) 1.07 (3H, t, J_{Hz} 7.5, $CH_2CCCH_2CH_3$); δ_{13C} (DMSO- d_6) 136.9, 124.4, 122.5, 90.2, 72.2, 39.3, 36.3, 13.7, 12.1; δ_{14N} (DMSO- d_6 ($\Delta_{1/2}$, Hz)) –131 (67), –207 (670), –276 (165). Found: C, 56.52; H, 6.84; N, 36.26. Calc. for $C_9H_{13}N_5$: C, 56.53; H, 6.85; N, 36.62.

1-Propargyl-3-methyl-imidazolium Azide (7). 1-Propargyl-3-methyl-imidazolium bromide (0.83 g) (4.13 mmol) and 15.73 g (59.77 mmol N_3^-) of azide exchange resin were reacted. Upon addition of the exchange resin, the solution turned dark brown. No unambiguous product was recovered.

In a modification to the general procedure, 0.38 g (1.89 mmol) of 1-propargyl-3-methyl-imidazolium bromide was added to a Schlenk flask and dissolved in ca. 30 mL of acetonitrile at +60 °C. After all of the material was dissolved, the solution was cooled in an ice bath for 30 min before adding 0.57 g (2.17 mmol N_3^-) of azide exchange resin. The solution was kept at 0 °C, but after a short period of time, the solution turned dark brown. Cold filtration again gave no isolable product.

1-Methyl-1,2,4-triazolium Nitrate (8). To a 25 mL glass reaction vessel equipped with a Kontes Teflon valve, ca. 3 mL of N_2O_4 was condensed at –196 °C. The valve was opened under a flow of dry nitrogen. A few milligrams of 1-methyl-4-amino-1,2,4-triazolium azide were added to the frozen N_2O_4 at –196 °C. The mixture was allowed to warm to ambient temperature in the open reaction vessel with dry nitrogen purge. After ambient conditions were attained, the valve was closed, and all volatiles were removed

in a dynamic vacuum leaving behind a crystalline white solid. Melting point (decomp.): +241 °C; Raman (500 mW, 25 °C, cm^{-1}) ν = 3127(13), 3036(18), 3022(20), 2963(24), 2878(4), 2805(6), 1647(2), 1564(7), 1472(10), 1443(11), 1419(11), 1403(7), 1365(31), 1264(7), 1245(7), 1159(4), 1120(19), 1079(5), 1040(100), 991(14), 928(12), 723(10), 715(7), 683(20), 674(24), 642(1), 375(5), 269(10), 148(31), 125(68), 102(67), 95(78), 85(85); δ_{1H} (MeOH- d_4) 9.66 (1H s), 8.78 (1H, s), 4.13 (3H, s, CH_3); δ_{13C} (MeOH- d_4) 145.6, 143.6, 38.7; δ_{14N} (DMSO- d_6 ($\Delta_{1/2}$, Hz)) –11 (18), –165 (215), –194 (238). Found: C, 24.62; H, 4.15; N, 38.26. Calc. for $C_3H_6N_4O$: C, 24.66; H, 4.14; N, 38.35.

X-ray Analyses. The single-crystal X-ray diffraction data were collected on a Bruker 3-circle-platform diffractometer equipped with a SMART detector with the χ -axis fixed at 54.74° and using Mo $K\alpha$ radiation (λ = 0.71073 Å) from a fine-focus tube. The diffractometer was equipped with a Kryoflex apparatus for low temperatures using controlled liquid nitrogen boil off. The goniometer head, equipped with a nylon Cryoloop and magnetic base, was used to mount the crystals using perfluoropolyether oil. Cell constants were determined from 90 ten-second frames, and a complete hemisphere of data was scanned on omega (0.3°) at 10 s per frame and a resolution of 512 × 512 pixels using the SMART software.^{14,15} A total of 2400 frames were collected in four sets, and final sets of 50 frames, identical to the configuration of the first 50 frames, were also collected to determine any crystal decay. The frames were then processed using the SAINT software^{16,17} to give the hkl file corrected for Lp/decay. The absorption correction was performed using the SADABS¹⁸ program. The structures were solved by the direct method using the SHELX-90¹⁹ program and refined by the least-squares method on F^2 , SHELXL-97²⁰ incorporated in SHELXTL Suite 5.10.^{21,22} All non-hydrogen atoms were refined anisotropically. For the anisotropic displacement parameters, the U(eq) is defined as one-third of the trace of the orthogonalized U_{ij} tensor. The hydrogen atoms were located either from difference electron density maps or generated at calculated positions.

Results and Discussion

Syntheses. The different azide salts (**1–6**, Scheme 1) were readily prepared using an azide-exchange resin as previously described.⁹ All salts are soluble in polar solvents such as acetonitrile, methanol, and water but are insoluble in diethyl ether, hexane, dichloromethane, and ethyl acetate. All salts were characterized by 1H , ^{13}C , and ^{14}N NMR, Raman spectroscopy, DSC, and elemental analysis. Viscosities were measured for liquid samples. The crystal structures of **5** and **8** were also determined.

All azides were easily identified by their characteristic symmetric-stretch vibration, $\nu_s N_3^-$. It is the most intense

(14) SMART, version 4.045; software for the CCD detector system; Bruker AXS, Inc.: Madison, WI, 1999.

(15) SMART for WNT/2000, version 5.625; Bruker AXS, Inc.: Madison, WI, 2001.

(16) SAINT, version 4.035; software for the CCD detector system; Bruker AXS, Inc.: Madison, WI, 1999.

(17) SAINT PLUS, version 6.22; Bruker AXS, Inc.: Madison, WI, 2001.

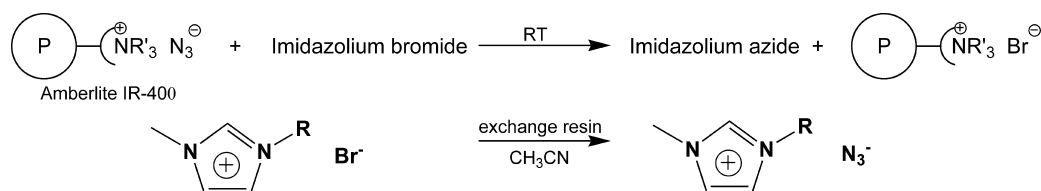
(18) SADABS, version 2.01; program for absorption correction for area detectors; Bruker AXS, Inc.: Madison, WI, 2000.

(19) Sheldrick, G. M. *SHELXS-90, Program for the Solution of Crystal Structure*, University of Göttingen, Germany, 1990.

(20) Sheldrick, G. M. *SHELXL-97, Program for the Refinement of Crystal Structure*; University of Göttingen, Germany, 1997.

(21) SHELXTL 5.10 for Windows NT, Program Library for Structure Solution and Molecular Graphics; Bruker AXS, Inc.: Madison, WI, 2000.

(22) SHELXTL, version 6.10; Bruker AXS, Inc.: Madison, WI, 2000.

Scheme 1^a

^a R = -butyl (1), -(2-hydroxyethyl) (2), -allyl (3), -(3-butenyl) (4), -(2-butenyl) (5), -(2-pentynyl) (6), and -propargyl (7).

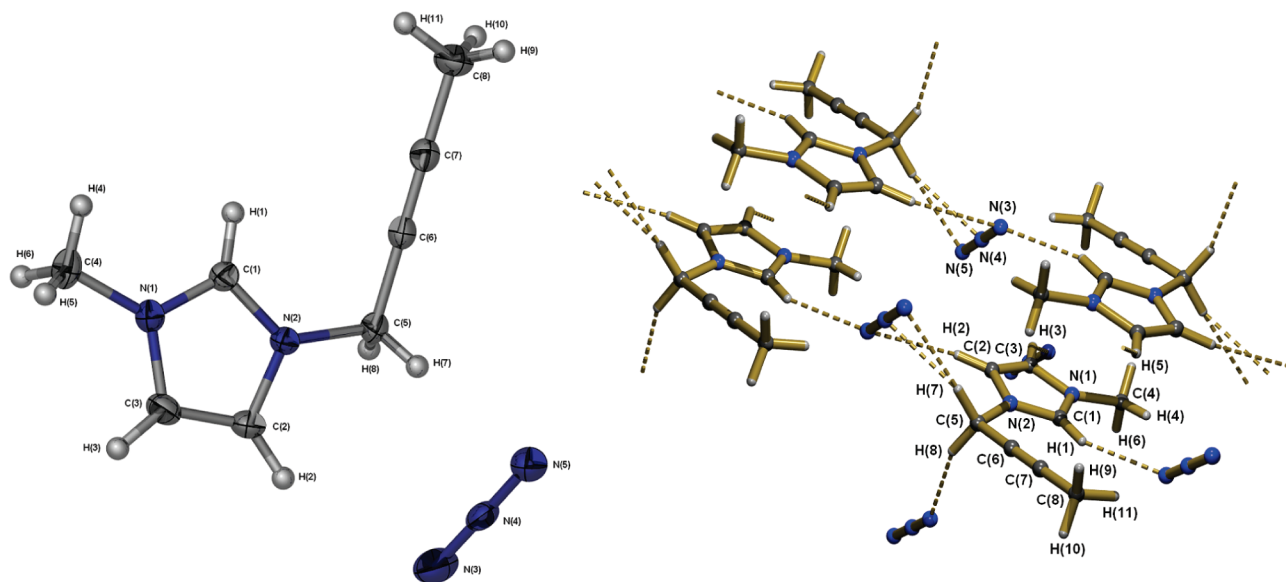


Figure 1. ORTEP diagram showing connectivity, conformation, and the atom numbering scheme of the individual cation and anion present in the asymmetric unit and the hydrogen-bond network of 1-(2-butenyl)-3-methyl-imidazolium azide (5).

Table 1. Physicochemical Properties of Imidazolium Azides and Reference Compounds

	imidazolium cation	$T_{g(\text{peak})}$ (°C)	$T_{m(\text{peak})}$ (°C)	$T_{\text{dec(onset)}}$ (°C)	η/cP (25 °C)	$\Delta_f H^\circ$ (kcal mol ⁻¹) ^c	$\Delta_c H^\circ$ (kcal g ⁻¹) ^c
1	1-butyl-3-methyl-	-74	+36	+222	404 ^a	+73	-7.38
2	1-(hydroxyethyl)-3-methyl	-3	+36	+214		+40	-5.79
3	1-allyl-3-methyl-	-77	+19	+150	201	+107	-6.91
4	1-(3-butenyl)-3-methyl-	-57	+45	+188	495 ^a	+101	-7.23
5	1-(2-butenyl)-3-methyl-		+66	+115		+143	-7.17
6	1-(2-pentynyl)-3-methyl-	-55	+19	+107	4124 ^b	+139	-7.47
	H ₂ NNH ₂ ^d					+12	-4.64
	MeN ₃ ^e					+71	-4.70
	HOCH ₂ CH ₂ N ₃ ^f					+22	-4.38

^a For supercooled liquid. ^b 0.5 rpm. ^c Solid phase (unless otherwise noted). ^d Liq. ref 38. ^e Gas ref 36. ^f Liq. ref 37.

band in the Raman spectra (except for lattice vibrations) and lies between 1318 cm⁻¹ and 1334 cm⁻¹. Lower frequencies indicate stronger hydrogen bonds with the substituent groups of the cation as can be seen, for example, in the crystal structure of **5** (Figure 1).

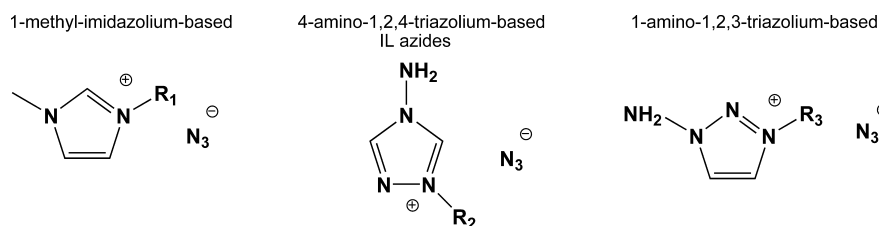
The attempted synthesis of 1-propargyl-3-methyl-imidazolium azide, **7**, did not result in an isolable product. One explanation might be the reaction between the azide resin and the terminal alkyne group. It is well established that alkynes undergo a 1,3-cycloaddition with azides yielding 1,4-substituted 1,2,3-triazoles.²³ These types of reactions are also referred to as click chemistry.²⁴ Intermediate triazoles could then undergo rapid thermal or photochemical reactions

forming various products. A characterization of these possible products was not a subject of this investigation.

Physical Properties. The melting, glass transition, and thermal decomposition temperatures determined by DSC are given in Table 1. Like their halide parents,¹³ the IL azides showed a tendency to form supercooled liquids and might be easily mistaken for true room-temperature ILs. Only after considerable time did some of the materials solidify and could their melting points be accurately measured. Melting points range from 19 °C for **6** up to 66 °C for **5**. Nearly all of the azides possess considerably lower melting points than the corresponding bromide salts. The most visible trend among the azides is a decrease in decomposition temperature

(23) Huisgen, R. *1,3-Dipolar Cycloaddition Chemistry*; Padwa, A., Ed.; Wiley: New York, 1984; Vol. 1, pp 1–176.

(24) Kolb, H. C.; Finn, M. G.; Sharpless, K. B. *Angew. Chem., Int. Ed.* **2001**, *40*, 2004.

Scheme 2^a

^a R₁ = -butyl, -allyl, -(3-butenyl), and -(2-pentynyl); R₂ = -methyl, -allyl, -(2-hydroxyethyl), and -(2-azidoethyl); R₃ = -allyl.

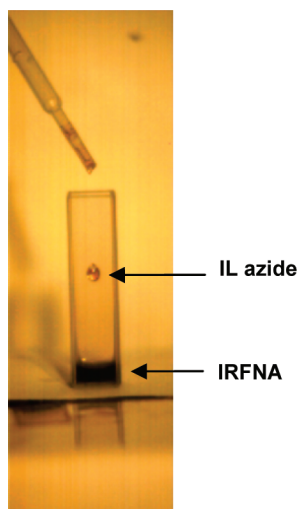


Figure 2. Shown is a typical experimental setup for a droplet experiment. The cuvette contains the oxidizer IRFNA or N₂O₄ to which an IL azide fuel droplet is added by means of a disposable pipet.

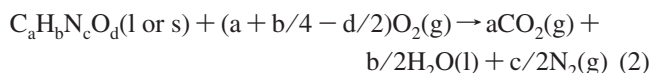
going from saturated to unsaturated side chains in the order of alkanes to alkenes to alkynes.

For ease of pumping and dispersal for combustion, it is desirable that propellants have low viscosities. Therefore, the viscosities of the room-temperature liquids or supercooled liquids were measured (Table 1). They range between 201 to 4124 cP, not unexpectedly large considering chain length and saturation of the pendant groups. Although some of the pure compounds are too viscous for propellant applications, it is expected that this might be remedied with suitable additives.

Another key feature is the heat of formation of the compounds. Theoretical performance can be estimated from calculated heats of formation. In general, a promising compound should possess a high positive heat of formation without inducing thermal instability or shock sensitivity. Table 1 lists the calculated solid-phase heats of formation for the compounds investigated. The enthalpy of melting for the liquids was neglected. For **2** and **3** the gas-phase heats of formation for the separate ions were calculated by the G2 method²⁵ using Gaussian 98.²⁶ For the other cations, these values were derived from MP2/6-31G(d)//HF/6-31G(d) enthalpies²⁷ from GAMESS,²⁸ experimental^{29–31} or G2 heats of formation of the other reactants, and the homodesmotic reactions given in the Supporting Information.

(25) Curtiss, L. A.; Raghavachari, K.; Trucks, G. W.; Pople, J. A. *J. Chem. Phys.* **1991**, *94*, 7221.

In all cases, the sum of the enthalpies of the ions was then corrected for the lattice enthalpy of a solid as estimated using the procedures described by Jenkins³³ with the individual crystal ion volumes approximated by the volumes enclosed by the 0.001 electron contour of the HF/6-31G(d) electron density in the isolated ion.^{34,35} The heats of combustion (Table 1) were then calculated according to eq 2.



For easier comparison, data for known compounds, CH₃N₃,³⁶ HOCH₂CH₂N₃,³⁷ and H₂NNH₂³⁸ are given as well.

Reactivity toward the Common Oxidizers IRFNA and N₂O₄. Most known energetic ILs consist of a heterocyclic cation and an oxygen-carrying anion,³⁹ and in bipropellant application, the cation would thus largely constitute the fuel. Consequently, the positively charged fuel portion

- (26) Frisch, M. J.; Trucks, G. W.; Schlegel, H. B.; Scuseria, G. E.; Robb, M. A.; Cheeseman, J. R.; Zakrzewski, V. G.; Montgomery, J. A., Jr.; Stratmann, R. E.; Burant, J. C.; Dapprich, S.; Millam, J. M.; Daniels, A. D.; Kudin, K. N.; Strain, M. C.; Farkas, O.; Tomasi, J.; Barone, V.; Cossi, M.; Cammi, R.; Mennucci, B.; Pomelli, C.; Adamo, C.; Clifford, S.; Ochterski, J.; Petersson, G. A.; Ayala, P. Y.; Cui, Q.; Morokuma, K.; Malick, D. K.; Rabuck, A. D.; Raghavachari, K.; Foresman, J. B.; Cioslowski, J.; Ortiz, J. V.; Stefanov, B. B.; Liu, G.; Liashenko, A.; Piskorz, P.; Komaromi, I.; Gomperts, R.; Martin, R. L.; Fox, D. J.; Keith, T.; Al-Laham, M. A.; Peng, C. Y.; Nanayakkara, A.; Gonzalez, C.; Challacombe, M.; Gill, P. M. W.; Johnson, B. G.; Chen, W.; Wong, M. W.; Andres, J. L.; Head-Gordon, M.; Replogle, E. S.; Pople, J. A. *Gaussian 98*, revision A.7; Gaussian, Inc.: Pittsburgh, PA, 1998.
- (27) Van Wazer, J. R.; Kellö, V.; Hess, B. A., Jr.; Ewig, C. S. *J. Phys. Chem.* **1990**, *94*, 5694.
- (28) Gordon, M. S.; Schmidt, M. W. *Theory and Applications of Computational Chemistry*; Dykstra, C. E., Frenking, G., Kim, K. S., Scuseria, G. E., Eds. Elsevier, Amsterdam, 2005.
- (29) Rogers, D. W.; Dagdagan, O. A.; Allinger, N. L. *J. Am. Chem. Soc.* **1979**, *101*, 671.
- (30) Wagman, D. D.; Kilpatrick, J. E.; Pitzer, K. S.; Rossini, F. D. *J. Res. NBS* **1945**, *35*, 467.
- (31) Pedley, J. B. *Thermochemical Data and Structures of Organic Compounds*; TRC; Chapman and Hall: New York, 1994; Vol. 1.
- (32) George, P.; Trachtman, M.; Brett, A. M.; Bock, C. W. *J. Chem. Soc., Perkin Trans.* **1977**, *2*, 1036.
- (33) Jenkins, H. D. B.; Tudela, D.; Glasser, L. *Inorg. Chem.* **2002**, *41*, 2364.
- (34) Murray, J. S.; Brinck, T.; Lane, P.; Paulsen, K.; Politzer, P. *J. Mol. Struct. (Theochem)* **1994**, *307*, 55.
- (35) Dixon, D. A.; Feller, D.; Christie, K. O.; Wilson, W. W.; Vij, A.; Vij, V.; Jenkins, H. D. B.; Olson, R. M.; Gordon, M. S. *J. Am. Chem. Soc.* **2004**, *126*, 834.
- (36) Rogers, D. W.; McLafferty, F. J. *J. Chem. Phys.* **1995**, *103*, 8302.
- (37) Fagley, T. F.; Klein, E.; Albrecht, J. F. *J. Am. Chem. Soc.* **1953**, *75*, 3104.
- (38) Schmidt, E. W. *Hydrazine and Its Derivatives*, 2nd ed., Wiley: New York, 2001; p 287.
- (39) Shreeve, J. M.; Singh, R. P.; Verma, R. D.; Meshri, D. T. *Angew. Chem., Int. Ed.* **2006**, *45*, 3584.

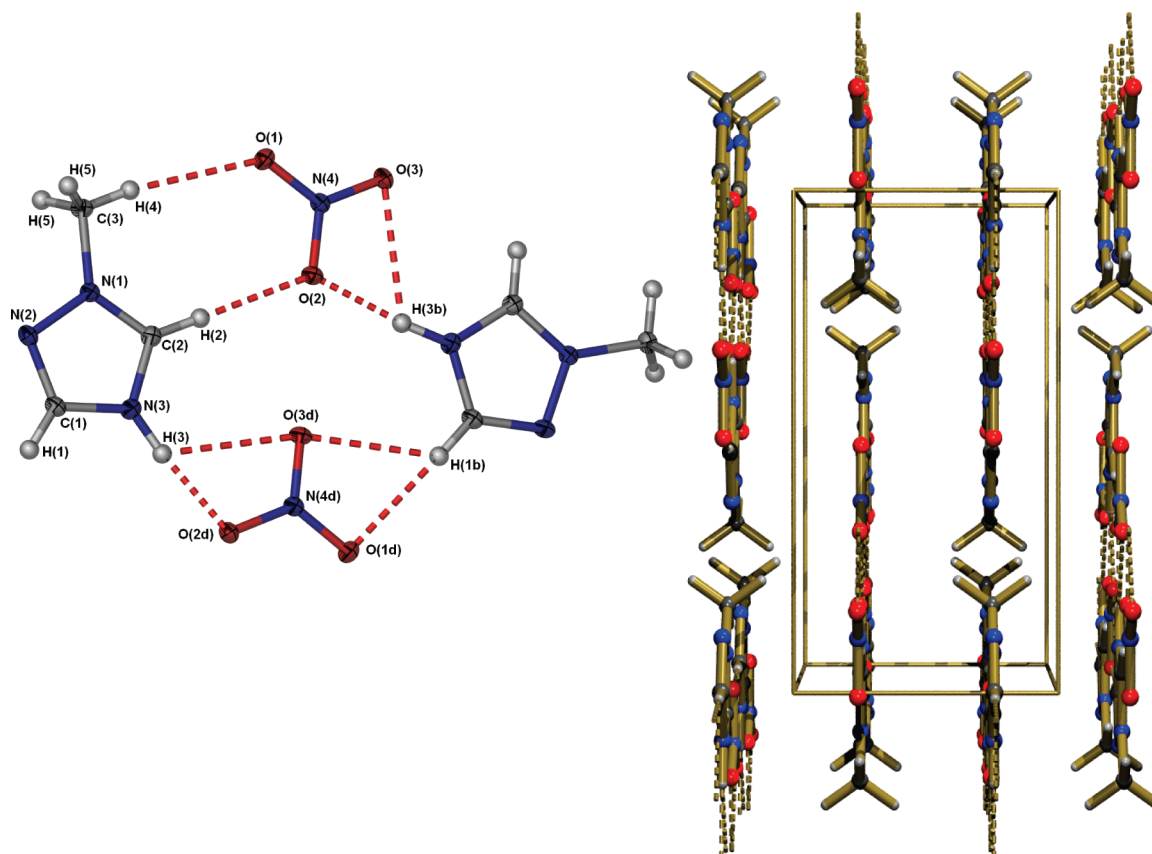


Figure 3. ORTEP diagram showing connectivity, conformation, and the atom numbering scheme of the individual cations and anions present in the asymmetric unit and packing diagram of 1-methyl-1,2,4-triazolium nitrate (**8**) along the *a* axis.

Table 2. Crystal and Structure Refinement Data for **5** and **8**^a

compound	1-(2-butynyl)-3-methyl-imidazolium azide (5)	1-methyl-1,2,4-triazolium nitrate (8)
formula	C ₈ H ₁₁ N ₅	C ₃ H ₆ N ₄ O ₃
space group	<i>P</i> $\bar{1}$ triclinic	<i>Pnma</i> orthorhombic
<i>a</i> (Å)	7.195(1)	9.115(5)
<i>b</i> (Å)	8.238(2)	6.141(4)
<i>c</i> (Å)	8.447(2)	10.967(7)
α (°)	68.765(3)	90.000
β (°)	89.253(3)	90.000
γ (°)	80.307(3)	90.000
<i>V</i> /Å ³	459.4(2)	613.9(7)
$\rho_{\text{calc.}}$ /g cm ⁻³	1.281	1.581
<i>Z</i>	2	4
formula weight	177.22	146.12
μ /mm ⁻¹	0.086	0.140
temperature (K)	173(2)	173(2)
λ (MoK α)	0.71073	0.71073
crystal size	0.30 \times 0.20 \times 0.10	0.60 \times 0.10 \times 0.10
theta range θ /°	2.59 to 28.61	2.91 to 28.46
index range	$-9 \leq h \leq 9$, $-10 \leq k \leq 10$, $-10 \leq l \leq 11$	$-9 \leq h \leq 11$, $-4 \leq k \leq 8$, $-13 \leq l \leq 14$
reflection collected	5484	2475
independent [R(int)]	2164 [0.016]	768 [0.032]
obs. refl. ($ I > 2.0 \sigma(I)$)	1980	704
F(000)	188	304
GooF	1.069	1.129
<i>R</i> ₁ , w <i>R</i> [$ I > 2\sigma(I)$]	0.0449, 0.1131	0.0387, 0.0871
<i>R</i> ₁ , w <i>R</i> ₂ (all data)	0.0487, 0.1156	0.0437, 0.1001
L.diff. peak/hole eÅ ³	0.25 and -0.18	0.31 and -0.30
absorption correct.	SADABS	SADABS
data/restraints/param.	2164/0/162	768/0/78
refinement method	full-matrix least-squares on <i>F</i> ²	full-matrix least-squares on <i>F</i> ²

$$^a R_1 = \Sigma |F_o| - |F_c| / \Sigma |F_o|; R_2 = \{\Sigma [w(|F_o|^2 - |F_c|^2)^2] / \Sigma [w(|F_o|^2)^2]\}^{1/2}.$$

is rendered more resistant toward oxidation, and this particular charge separation should lead to greater stability along with the other well-known advantages of ILs (low

vapor toxicity, consequent of low vapor pressure, etc.). However, this could also be a drawback for propulsion because of the greater expected resistance toward oxidation

Table 3. Selected Hydrogen Contact Lengths in Å of **5** and **8**

salt	hydrogen contact	length
5	H(1)⋯N(3)	2.32(2)
	H(7)⋯N(5)	2.44(2)
	H(7)⋯N(4)	2.45(2)
	H(8)⋯N(3)	2.33(2)
8	H(3)⋯O(2)	1.79(3)
	H(3)⋯O(3)	2.54(3)
	H(1)⋯O(1)	2.39(3)
	H(1)⋯O(3)	2.51(2)
	H(2)⋯O(2)	2.19(3)
	H(4)⋯O(1)	2.51(3)

and resulting difficulty in achieving rapid (<5 ms) hypergolic ignition. Although oxidizer anions contribute to the overall performance (i.e., density and oxygen balance), they do not necessarily help with hypergolic ignition (as an extensively oxidized anion would not be expected to participate in oxidative preignition reactions).

Consequently, in the present investigation, unsaturated hydrocarbon trigger groups on the cation were combined with azide anions, in an effort to promote hypergolicity. Scheme 2 shows all tested IL azides. A typical experimental setup is shown in Figure 2. With IRFNA and N₂O₄, all compounds reacted vigorously with copious production of red fumes, but without ignition. Under the same test conditions, hydrazine and its derivative monomethylhydrazine always spontaneously ignited.¹⁴ N NMR investigations of the residues revealed the formation of nitrates as suggested by eq 1. Volatile products were collected and examined using FTIR spectroscopy. With both oxidizers, N₂O was observed, consistent with eq 1 and the fact that IRFNA contains significant quantities of N₂O₄ (IRFNA = 83% HNO₃ + 14% N₂O₄ + 1.5–2.5% H₂O + 0.6% HF). Treatment with IRFNA also led to the observation of HN₃, produced by a displacement of the weaker acid from its salt.

The reaction of 1-methyl-4-amino-1,2,4-triazolium azide with N₂O₄ was additionally investigated under more gentle conditions than the drop tests. The solid residue, which was left behind after reaction with N₂O₄ and removal of all volatiles, was recrystallized from methanol layered with diethylether and identified as the new salt, 1-methyl-1,2,4-triazolium nitrate, **8**, by its Raman and NMR spectra and from single crystal X-ray investigation (Figure 3). This deaminated nitrate indicates that in these fuels both cation and anion participate in the oxidative reaction. It appears, however, that at these reaction conditions the initial heat release was not sufficient to further decompose the heterocyclic intermediates and yield hypergolic ignition, even when more reactive sidechains than a simple methyl group were built into the compound. The relatively large droplets may lack a sufficient surface-area-to-volume ratio, and in this configuration (Figure 2), the oxidizer should be expected to serve as a heat sink. Nevertheless, under the same conditions, experiments carried out with hydrazine always led to rapid hypergolic ignition. Because it is broadly accepted that ignition in known hypergolic systems takes place in the gas phase,⁴⁰ and one of the characteristics of ionic liquids is their

low vapor pressure, further ignition experiments are considered to determine if finely dispersed droplets, in conditions more similar to existing engines, will ignite.

Crystal Structure Determination of 1-(2-Butynyl)-3-methyl-imidazolium Azide (5) and 1-Methyl-1,2,4-triazolium Nitrate (8). Single crystals of **5** were obtained from methanol layered with diethylether. Compound **5** crystallized in the triclinic space group *P* $\bar{1}$ (Table 2). Figure 1 shows both the individual cation and anion, and the hydrogen-bonded network. The packing arrangement in the unit cell consists of two identical cation layers rotated by 180° and separated by azide anions. The pendant 2-butynyl group is bent away from the imidazolium ring by 111.2° (N(2)–C(5)–C(6)), but lies almost in its plane, showing only a small dihedral twist of 17.4° (C(1)–N(2)–C(5)–C(6)). This twist is 10° larger than in the corresponding bromide salt,¹³ attributable to hydrogen bonding with the azide anions. The azide anion shows four contacts (2.32 Å to 2.45 Å), which are more than 10% shorter than the sum of the Van der Waals radii (2.75 Å) (Table 3).⁴¹ Three of these contacts involve the CH₂-protons and one the H(1) ring proton. A longer hydrogen bond, 2.55 Å, is formed between N(5) of the azide anion and H(3) of the ring. In fact, these regions correspond to local maxima on the calculated electrostatic potential of the cation at the constant electron density contour as shown in the Supporting Information. Three very weak contacts involve the methyl protons (2.68 Å and 2.70 Å) and the H(2) ring proton (2.63 Å).

Compound **8** crystallized in an orthorhombic space group *P*_{mma} (Table 2). Figure 3 shows the individual cation and anion, and the hydrogen-bond network. Note that H(3) has replaced the amino group, which was attached to N(3) prior to the reaction with N₂O₄. The overall packing is dominated by attractive Coulomb forces accompanied by substantial hydrogen bonding from ring- and methyl-hydrogens to the nitrate anion. The packing arrangement consists of well-defined layers of alternating cations and anions. Within these layers, alternating cations are rotated by 90°, and the view along the *a* axis demonstrates how the cations and anions are connected via hydrogen bonds. Figure 3 also shows that there are no contacts between the clearly separated layers. Hydrogen bonding dominates the structure, and the shortest contacts are listed in Table 3. A remarkably strong hydrogen bond of only 1.79(3) Å connects the proton on the ring nitrogen to a nitrate oxygen (H(3)⋯O(2)). Indeed, the calculation for the isolated cation indicates that this region is highly electropositive (see Supporting Information).

Conclusions

The series of known IL azides was expanded by synthesizing methylimidazolium heterocycles with saturated and unsaturated side chains. Their reactivity toward strong oxidizers (IRFNA and N₂O₄) was investigated. In the case of the amino-triazolium salts, it was successfully demonstrated that both parts of the fuel, cation and anion, can react with the oxidizer. Unfortunately, the initial heat release

(40) Alfano, A. J.; Mills, J. D.; Vaghjiani, G. L. *Rev. Sci. Instrum.* **2006**, 77, 045109–1.

(41) Bondi, A. J. *Phys. Chem.* **1964**, 68, 441.

during these reactions did not result in hypergolic ignition of the material under the tested conditions. The results are sufficiently encouraging to justify the expectation that variations in test conditions and ILs may lead to a practical IL hypergol.

Acknowledgment. We thank AFOSR (Mike Berman) for financial support of this work.

Supporting Information Available: Crystallographic data for **5** and **8** in CIF format. The homodesmic reactions for the calculation of the gas-phase heats of formation of the cations of **1**, **4**, **5**, and **6**, and calculated electrostatic potential surfaces for the cations of **5** and **8**. This material is available free of charge via the Internet at <http://pubs.acs.org>.

IC8004739